

## INVESTIGATION OF STRUCTURE AND PROPERTIES OF BARRIER LAYERS IN METALS (Fe, Cu) AT LOW TEMPERATURES

K. A. Kuterbekov,<sup>1</sup> S. A. Nurkenov,<sup>1</sup> S. B. Kislitsin,<sup>2</sup>  
T. A. Kuketayev,<sup>3</sup> and A. K. Tussupbekova<sup>3</sup>

UDC 539.172:539.2:539.26

*Experimental studies of the effect of a barrier layer on the kinetics of thermally induced diffusion processes and phase transformations in a layered Fe–Be system are investigated at the energy  $\sim 1.6$  MeV. Thermal stability of the barrier layer in the Fe:O<sup>+</sup> system is validated and a possibility of its use as a subsurface layer for a beryllium coating is demonstrated. For the Cu:O<sup>+</sup> system it is shown that the implanted layer in the matrix comes apart already at the annealing temperature  $\sim 180^\circ\text{C}$  and could not be used in a copper matrix as a subsurface barrier layer. For the first time, a method is proposed for retardation of diffusion and phase formation processes and realized in a layered iron – beryllium system using an implanted layer of oxygen ions. The sequence and characteristic times of thermally-induced phase-transformation processes taking place in the subsurface layers and in the bulk of the Fe (10  $\mu\text{m}$ ) systems: O<sup>+</sup> – Be (0.7  $\mu\text{m}$ ) – <sup>57</sup>Fe (0.1  $\mu\text{m}$ ) and Fe (10  $\mu\text{m}$ ) – Be (0.7  $\mu\text{m}$ ) – <sup>57</sup>Fe (0.1  $\mu\text{m}$ ) are determined.*

**Keywords:** oxygen ion implantation, barrier layer, thermal stability, phase transformations.

### INTRODUCTION

The development of new efficient processes for engineering materials operating in aggressive media under conditions of thermal, radiation and other stresses is an urgent task of modern materials science [1].

At present, a good deal of attention is given to the metal – metalloid implantation system, since by forming an interstitial phase in the subsurface layers of an irradiated metal it is possible to improve its strength and corrosion-resistant properties. The data of these investigations could be used in practice via formation of heat-resistant coatings on the specimens, thus new technological methods have to be developed for deposition of high-temperature protective coatings [1, 2].

In this study we propose to form barrier coatings using ion implantation processes. A successive implementation of ion implantation and plasma-assisted ion sputtering results in the formation of a layered system representing a matrix with a subsurface barrier layer and a protective coating. In accordance with the experimental design, we put forward the following tasks: i) to form barrier coatings in metals, Cu and Fe, by implanting oxygen ions and investigate their stability; ii) to study the influence of the resulting barrier layer on the kinetics of thermally-induced diffusion and phase formation in the layered systems in question; iii) to determine the relative phase content and routes of phase transformations in the subsurface layers and in the bulk of layered systems under conditions of successive isothermal annealing; iv) to implement the method of deceleration of diffusion and phase formation

---

<sup>1</sup>L. N. Gumilyov Eurasian National University, Astana, Republic of Kazakhstan, e-mail: kkuterbekov@gmail.com; S.Nurkenov@gmail.com; <sup>2</sup>Institute of Nuclear Physics, Almaty, Republic of Kazakhstan, e-mail: skislitsin@mail.ru; <sup>3</sup>Y. A. Buketov Karaganda State University, Karaganda, Republic of Kazakhstan, e-mail: katkargu@mail.ru. Translated from *Izvestiya Vysshikh Uchebnykh Zavedenii, Fizika*, No. 7, pp. 59–64, July, 2016. Original article submitted October 23, 2015; revision submitted February 24, 2016.

TABLE1. Characteristics and Irradiation Conditions

No.	Specimens	Specimen thickness	Implanted ion	Accelerator type	Irradiation energy	Ion fluence, ion/cm <sup>2</sup>	Ion path length <i>R</i> , nm
1	Cu	1 mm	O <sup>+</sup>	DC-60 (Astana)	100 keV	2·10 <sup>18</sup>	290
2	Fe ( $\alpha$ -iron)	10 $\mu$ m	O <sup>+</sup>	UKP-2-1 (Almaty)	1.6 MeV	1.1·10 <sup>18</sup>	950

processes in the layered systems formed using a barrier coating; and v) to develop an approach for reconstruction of the distribution function of the impurity atom concentration in the matrix – impurity solid solution using the X-ray diffraction data, and realized them in this study.

## ANALYTICAL PROCEDURES

The analytical techniques included Mössbauer spectroscopy (MS) with registration of  $\gamma$ -quanta in the transmission-mode geometry, conversion electron Mössbauer spectroscopy (CEMS) in the backscattering geometry, and Rutherford backscattering (RBS) of protons. These methods were chosen for the following reasons: MS provides information on the phase state averaged over the specimen thickness, CEMS provides data from the specimen subsurface layer  $\sim 0.1 \mu\text{m}$  and in the bulk (down to  $\sim 3 \mu\text{m}$ ), and RBS allows determining the oxygen penetration depth into Fe with respect to the specimen thickness [3–5].

Preparation of the specimens for analysis was carried out in a standard vacuum furnace (at  $P = 5 \cdot 10^{-6}$  mm Hg), the time to achieve the specified temperature was  $\sim 30$  min, the specimens cooled together with the furnace, and the temperature measurement error was within  $\pm 5^\circ\text{C}$ . The substrate thickness was determined by a conventional micrometer, its measurement error being  $\pm 1 \mu\text{m}$ . The specimens after their preparation (rolling) for investigations were subjected to thermal annealing at the temperature  $850^\circ\text{C}$  for 3 hours. The experiments on irradiation of thus prepared specimens were performed using the UKP-2-1 (NPI at the NNC, Almaty) and DC-60 (Gumilyov ENU, Astana) facilities. At every stage of the experiments, after annealing the specimens were examined by CEMS of  $^{57}\text{Fe}$  nuclei, X-ray phase analysis and RBS of protons.

After thermal annealing of the  $\alpha$ -Fe (10  $\mu\text{m}$ ) specimens without oxygen and with implanted oxygen layer, a  $0.7 \mu\text{m}$  layer of beryllium was deposited on them using the plasma-ion process. In order to improve sensitivity of the Mössbauer spectroscopy procedures, a  $\text{Fe}^{57}$ -enriched layer  $\sim 0.1 \mu\text{m}$  thick was formed using a PVD method. Thermal annealing of these systems was performed in a standard-design vacuum furnace at the temperature  $T = 700^\circ\text{C}$ , the annealing time was counted from the point  $\tau = 0.5$  hour with the time step being  $\Delta\tau = 2.5$  hours. The annealing modes were selected taking into account the phase diagram features of the Fe:O<sup>+</sup> and Fe–Be systems [5–9].

## RESULTS AND DISCUSSION

Figure 1 presents an RBS spectrum from the specimen prior to and after implantation and a profile of the barrier layer distribution in the iron matrix obtained in the UKP-2-1 accelerating charge-exchange complex.

During the experiments we determined the depth of oxygen penetration into the  $\alpha$ -Fe matrix and the oxygen concentration over the specimen depth after implantation.

Let the number of ion (proton) energy loss per unit length be equal to  $dE/dx$ . Then the total energy loss  $\Delta E$ , for the ion reaching depth  $t$ , would be proportional to  $t$

$$\Delta E = \int_0^t (dE / dx) dx \approx dE / dx |_{\text{in}} t ,$$

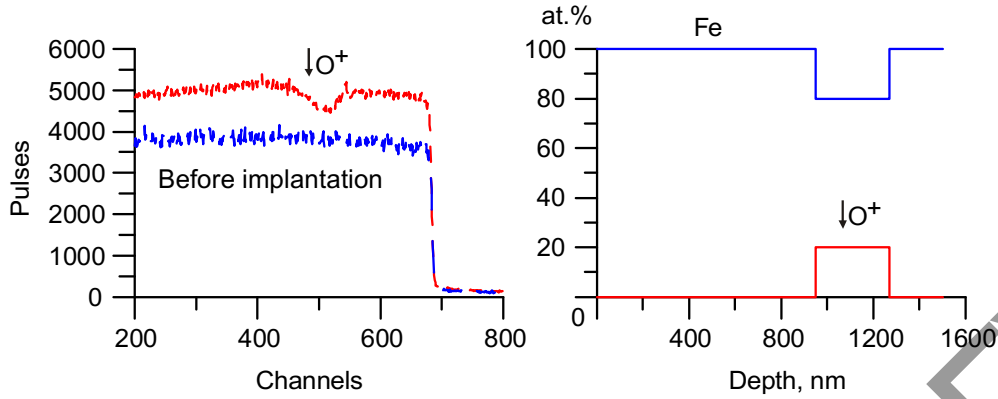


Fig. 1. RBS spectrum from the specimen prior to and after implantation and a profile of the barrier layer distribution in the iron matrix.

where  $dE/dx|_{in}$  is the energy loss of a particle before dissipation calculated for the average energy between the initial  $E_0$  and  $E_0 - t(dE/dx)$ . At depth  $t$ , the particle has the energy given by

$$E(t) = E_0 - t dE / dx |_{in}$$

After dissipation within a large angle, the particle's energy becomes equal to  $kE(t)$ , where the kinematic multiplier  $k$  is found from the following formula:

$$k = [(M_1 \cos\theta + (M_2^2 - M_1^2 \sin^2\theta)^{1/2}) / (M_1 + M_2)].$$

Here  $M_1$ ,  $M_2$  are the ion (proton) and target nucleus masses, respectively, and  $\theta$  is the scattering angle. The measured scattered ion energies at a known scattering angle  $\theta$  allow us to determine  $M_2$ . Having changed the direction of its motion, the particle keeps on decelerating in its return path towards the detector; it reaches the latter having the energy

$$E_1(t) = kE(t) - (t/\cos\theta)dE/dx|_{out} = -t(kdE/dx|_{in} + (1/\cos\theta)dE/dx|_{out}) + kE_0.$$

Then the spectral width of the energy  $\Delta E$  of particles, backscattered by the film of width  $\Delta t$ , would be equal to

$$\Delta E = \Delta t (kdE/dx|_{in} + (1/\cos\theta)dE/dx|_{out}).$$

Backscattering spectrometry allows determining compositional changes with the depth. The relationship between the energy resolution  $\delta E_1$  and the depth resolution  $\delta t$  is given by

$$\delta t = \delta E_1 / (kdE/dx|_{in} + (1/\cos\theta)dE/dx|_{out}).$$

The best depth sensitivity is found in the case of maximum energy losses accompanying scattering in the bulk of the specimen. This is achieved by the use of grazing-incidence small-angle scattering, which ensures a depth resolution of 2 nm with conventional semiconductor detectors. In the latter case, such factors affecting the resolving power as the end capture angle of the detector, surface roughness, and energy straggling have to be taken into account. The resolving power variations are minimal at the angle  $\theta = 180^\circ$ . The difference between the particles backscattered from the elements with different values of  $Z$  is also maximal at the scattering angle  $180^\circ$ . It is for this reason that backscattering spectrometry is commonly implemented at the values of  $\theta$  close to  $180^\circ$ . In this case, the energy variance introduced by the limited solid angle of the detector is minimal, while the capacity of discriminating the specimen atoms with different masses is maximal. Recently, specialized surface-barrier detectors have been developed, which

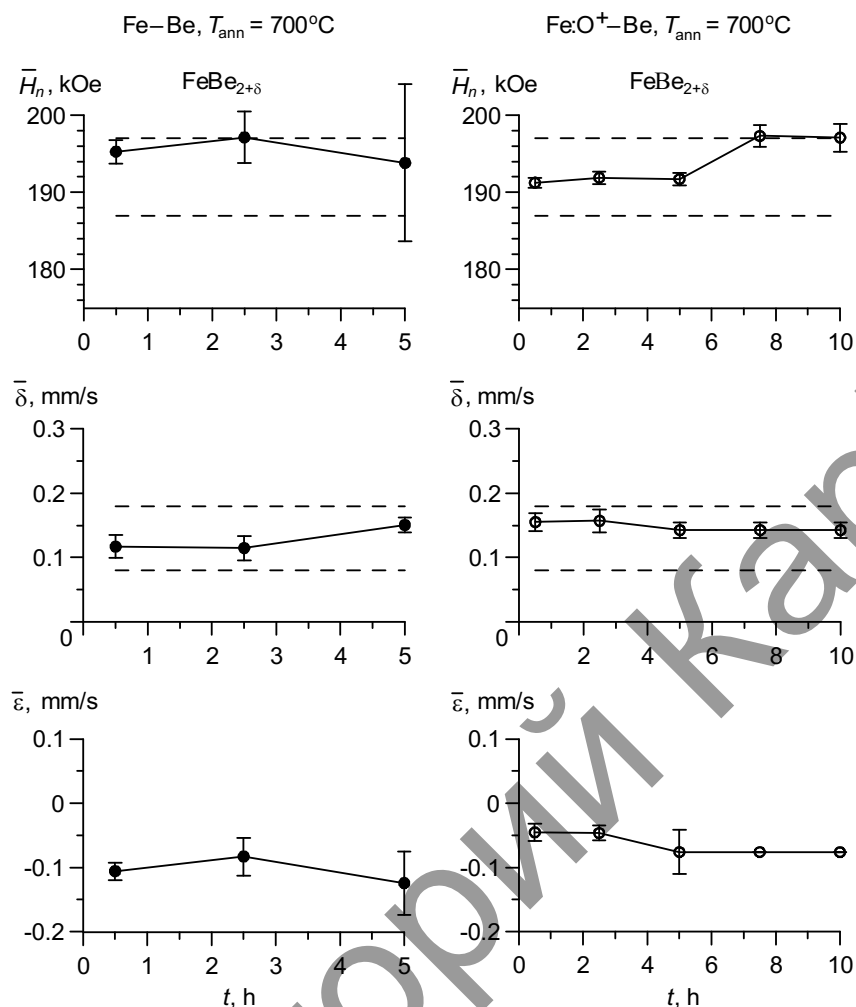


Fig. 2. Average values of the effective magnetic fields  $H_n$ , shears  $\delta$  and quadrupole displacements  $\epsilon$  of the Mössbauer spectra for the  $\text{FeBe}_{2+\delta}$ -phase in  $\text{Fe-Be-}^{57}\text{Fe}$  and  $\text{Fe:O}^+-\text{Be-}^{57}\text{Fe}$  as a function of the isothermal annealing time  $t_{\text{ann}}$  at  $T_{\text{ann}} = 700^\circ\text{C}$ .

have an opening in the center for the beam. The spectra of backscattered ions and the element distribution over the specimen depth were processed and analyzed by the RBS-technique using the RUMP simulator. The RUMP concentration profile of elements is represented as an interchange of layers of varied thicknesses and compositions, wherein the concentration of elements is prescribed as a stoichiometric formula. The number of layers of similar compositions is limited to 100, while the number of elements per layer is unlimited. In addition to simulations of the theoretical spectrum and the online fitting procedure, this software makes it possible to autofit the theoretical spectrum to the experimental one having no more than eight variable parameters. The error in the case of film thickness determination using autofit is as low as  $\Delta t/t \approx 6\%$ .

Using the MS analytical data, we calculated the average values of the effective magnetic fields  $H_n$ , shears  $\delta$ , and quadrupole displacements  $\epsilon$  of the MS spectra for the  $\text{FeBe}_{2+\delta}$ -phase in the layered  $\text{Fe-Be-}^{57}\text{Fe}$  and  $\text{Fe:O}^+-\text{Be-}^{57}\text{Fe}$  systems as a function of isothermal annealing time  $t_{\text{ann}}$  at the temperature  $T_{\text{ann}} = 700^\circ\text{C}$  (Fig. 2). The Mössbauer values of superfine parameters are consistent with the data obtained in [7]. The dash-line boundaries in Fig. 2 indicate the values reported in the literature.

In order to determine the characteristic time of the  $\text{FeBe}_{2+\delta} \rightarrow \text{Fe(Be)}$  phase transformation, the following kinematic equation was proposed:

TABLE 2. Parameters of Mössbauer Spectra for FeBe<sub>2+δ</sub> after Isothermal Anneals at  $T_{\text{ann}} = 700^{\circ}\text{C}$

$t_{\text{ann}}, \text{h}$	Fe-Be- <sup>57</sup> Fe				Fe:O <sup>+</sup> -Be- <sup>57</sup> Fe			
	$\delta, \text{mm/s}$	$\varepsilon, \text{mm/s}$	$H_n, \text{kOe}$	$I, \%$	$\delta, \text{mm/s}$	$\varepsilon, \text{mm/s}$	$H_n, \text{kOe}$	$I, \%$
0.5	$0.112 \pm 0.01$	$-0.102 \pm 0.03$	$195.3 \pm 1.5$	$3.8 \pm 0.7$	$0.154 \pm 0.01$	$-0.058 \pm 0.02$	$191.2 \pm 0.6$	$13.8 \pm 0.9$
2.5	$0.115 \pm 0.01$	$-0.083 \pm 0.03$	$197.1 \pm 0.7$	$1.1 \pm 0.7$	$0.155 \pm 0.04$	$-0.074 \pm 0.06$	$191.1 \pm 0.8$	$11.4 \pm 0.7$
5.0	$0.145 \pm 0.01$	$-0.164 \pm 0.03$	$195.4 \pm 1.1$	$0.5 \pm 0.5$	$0.145 \pm 0.01$	$-0.050 \pm 0.03$	$191.7 \pm 0.8$	$3.9 \pm 0.7$
7.5	–	–	–	–	$0.143^*$	$-0.076^*$	$197.3 \pm 1.4$	$0.7 \pm 0.2$
10.0	–	–	–	–	$0.143^*$	$-0.076^*$	$197.1 \pm 1.8$	$0.9 \pm 0.5$
15.0	–	–	–	–	–	–	–	–

Note.  $\delta_{\text{max}}, \varepsilon_{\text{max}}$  are the Mössbauer line shear and quadrupole displacement, corresponding to the maximum value of the distribution function,  $H_n$  is the superfine magnetic field,  $I$  is the intensity, and an asterisk \* marks the values fixed during spectrum processing.

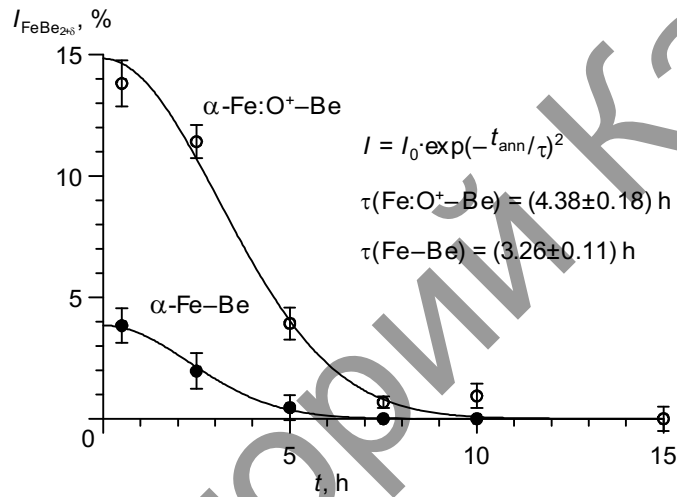


Fig. 3. Partial spectral intensities of the FeBe<sub>2+δ</sub>-phase in the Fe-Be-<sup>57</sup>Fe and Fe:O<sup>+</sup>-Be-<sup>57</sup>Fe layered systems versus the time of isothermal annealing at  $t_{\text{ann}}$  at  $T_{\text{ann}} = 700^{\circ}\text{C}$ .

$$I(t_{\text{ann}}) = I_0 \exp\left(-\frac{t_{\text{ann}}}{\tau}\right)^2,$$

where  $I_0$ , the partial spectral intensity, is a constant value,  $\tau$  is the characteristic time of variation of the relative partial spectral intensity of the FeBe<sub>2+δ</sub>-phase, and  $t_{\text{ann}}$  is the time of isothermal annealing.

Having processed the  $I(t_{\text{ann}})$  curves using the MSTools KINETIC software program [8, 9], we obtained the following values of the kinetic equation parameters for the systems with and without barrier layers:  $\tau(\text{Fe:O}^+-\text{Be}) = (4.38 \pm 0.18) \text{ h}$  and  $\tau(\text{Fe-Be}) = (3.26 \pm 0.11) \text{ h}$ , respectively.

Figure 3 depicts for the Fe-Be-<sup>57</sup>Fe and Fe:O<sup>+</sup>-Be-<sup>57</sup>Fe layered systems the plots of relative partial spectral intensities of the FeBe<sub>2+δ</sub>-phase for the <sup>57</sup>Fe nuclei versus the anneal time  $t_{\text{ann}}$  at the temperature  $T_{\text{ann}} = 700^{\circ}\text{C}$ . These plots validate a complete solution of the FeBe<sub>2+δ</sub>-phase followed by the formation of a solid solution of beryllium in the iron matrix.

Table 2 presents the Mössbauer parameters of the respective spectra for the FeBe<sub>2+δ</sub>-phase after isothermal anneals at  $T_{\text{ann}} = 700^{\circ}\text{C}$ .

## SUMMARY

As a result of investigations by the methods of Mössbauer spectroscopy on the  $^{57}\text{Fe}$  nuclei and Rutherford backscattering of protons it has been established that a barrier layer affects the kinetics of thermally induced diffusion and phase transformation processes in a layered Fe–Be system. The Fe:O<sup>+</sup> system, using which the method of deceleration of diffusion and phase transformation processes in a layered iron – beryllium system was realized, has been found to be stable. It has been shown that the barrier layer restricts the zone of beryllium solution in the subsurface layer. For the first time, we have proposed and implemented the method of deceleration of diffusion and phase transformations in a layered iron – beryllium system using an implanted layer of oxygen ions. The sequence and characteristic times of thermally-induced FeBe<sub>2+δ</sub> → α-Fe(Be) phase transformations in the subsurface layers and in the bulk of the Fe (10 μm): O<sup>+</sup> – Be (0.7 μm) –  $^{57}\text{Fe}$  (0.1 μm) and Fe (10 μm) – Be (0.7 μm) –  $^{57}\text{Fe}$  (0.1 μm) systems have been determined.

## REFERENCES

1. K. K. Kadyrzhanov, F. F. Komarov, A. D. Pogrebnyak, *et al.*, Ion-Beam and Ion-Plasma Modification of Materials [in Russian], Moscow, MSU (2005).
2. K. K. Kadyrzhanov, T. E. Turkebaev, and A. L. Udovskii, Physical Principles of Ion Technologies for Designing Multi-Layer Metallic Materials [in Russian], Almaty (2001).
3. K. K. Kadyrzhanov, V. S. Rusakov, S. A. Nurkenov, and S. B. Kislitsin, in: Proc. 7th Int. Conf. Interaction of Radiation with Solids, Minsk, Belarus (2007).
4. K. K. Kadyrzhanov, V. S. Rusakov, S. A. Nurkenov, and S. B. Kislitsin, in: Proc. 4th Eurasian Conference on Nuclear Science and its Application, Baku (2006).
5. S. A. Nurkenov, S. B. Kislitsin, K. A. Kuterbekov, *et al.*, Int. Conf. Young Scientists Science and Education, in: Proc. L.N. Gumilyov ENU, Astana (2008).
6. K. Kuterbekov, S. Kislitsin, and T. Nurachmetov, Nanomaterials: Applications and Properties, **1**(II), 397–401 (2011).
7. K. Ohta, J. Appl. Phys., **39**, No. 4, 2123–2126 (1968).
8. V. S. Rusakov, Bull. RAS. Physics, **63** (7), 1389–1396 (1999).
9. V. S. Rusakov, Mössbauer Spectroscopy of Locally Inhomogeneous Systems [in Russian], Almaty (2000).